AMERICAN JOURNAL OF PHYSIOLOGY
ENDOCRINOLOGY AND METABOLISM

Am J Physiol Endocrinol Metab 325: E661–E671, 2023.
First published October 25, 2023; doi:10.1152/ajpendo.00065.2023

RESEARCH ARTICLE

The metabolic benefits of substituting sucrose for maple syrup are associated with a shift in carbohydrate digestion and gut microbiota composition in high-fat high-sucrose diet-fed mice

Arianne Morissette,[1,2] Diana Majolli André,[1,2] Anne-Laure Agrinier,[1,2] Thibault V. Varin,[2] Geneviève Pilon,[1] Nicolas Flamand,[1,3] Vanessa P. Houde,[1] and André Marette[1,2]

[1]*Department of Medicine, Faculty of Medicine, Québec Heart and Lung Institute, Université Laval, Pavilion Marguerite d'Youville, Québec City, Québec, Canada;* [2]*Institute of Nutrition and Functional Foods (INAF), Université Laval, Québec City, Québec, Canada; and* [3]*Canada Excellence Research Chair on the Microbiome-Endocannabinoidome Axis in Metabolic Health (CERC-MEND), Université Laval, Québec City, Québec, Canada*

Abstract

Overconsumption of added sugars is now largely recognized as a major culprit in the global situation of obesity and metabolic disorders. Previous animal studies reported that maple syrup (MS) is less deleterious than refined sugars on glucose metabolism and hepatic health, but the mechanisms remain poorly studied. Beyond its content in sucrose, MS is a natural sweetener containing several bioactive compounds, such as polyphenols and inulin, which are potential gut microbiota modifiers. We aimed to investigate the impact of MS on metabolic health and gut microbiota in male C57Bl/6J mice fed a high-fat high-sucrose (HFHS + S) diet or an isocaloric HFHS diet in which a fraction (10% of the total caloric intake) of the sucrose was substituted by MS (HFHS + MS). Insulin and glucose tolerance tests were performed at 5 and 7 wk into the diet, respectively. The fecal microbiota was analyzed by whole-genome shotgun sequencing. Liver lipids and inflammation were determined, and hepatic gene expression was assessed by transcriptomic analysis. Maple syrup was less deleterious on insulin resistance and decreased liver steatosis compared with mice consuming sucrose. This could be explained by the decreased intestinal α-glucosidase activity, which is involved in carbohydrate digestion and absorption. Metagenomic shotgun sequencing analysis revealed that MS intake increased the abundance of *Faecalibaculum rodentium*, *Romboutsia ilealis*, and *Lactobacillus johnsonii*, which all possess gene clusters involved in carbohydrate metabolism, such as sucrose utilization and butyric acid production. Liver transcriptomic analyses revealed that the cytochrome P450 (Cyp450) epoxygenase pathway was differently modulated between HFHS + S- and HFHS + MS-fed mice. These results show that substituting sucrose for MS alleviated dysmetabolism in diet-induced obese mice, which were associated with decreased carbohydrate digestion and shifting gut microbiota.

NEW & NOTEWORTHY The natural sweetener maple syrup has sparked much interest as an alternative to refined sugars. This study aimed to investigate whether the metabolic benefits of substituting sucrose with an equivalent dose of maple syrup could be linked to changes in gut microbiota composition and digestion of carbohydrates in obese mice. We demonstrated that maple syrup is less detrimental than sucrose on metabolic health and possesses a prebiotic-like activity through novel gut microbiota and liver mechanisms.

gut microbiota; insulin resistance; liver steatosis; maple syrup; obesity

INTRODUCTION

Obesity represents a major health challenge, as it substantially increases the risk of metabolic disorders (1). In 2020, more than 15% of the adult population worldwide was considered obese (body mass index $\geq$ 30 kg/m^2), and this proportion is estimated to increase to 18% by 2030 (2). The consequences of this alarming situation are an ever-growing number of patients with type 2 diabetes, cardiovascular diseases, nonalcoholic fatty liver diseases, and cancer (3). It is now greatly recognized that the chronic overconsumption of added sugars, mostly in the form of sugar-sweetened beverages (SSBs) (4), is a major culprit in this obesity pandemic (5, 6). As a matter of fact, several scientific organizations such as the World Health Organization (WHO), the American Heart Association, and the Institute of Medicine have developed recommendations for an upper daily limit of added or free sugars. The WHO recommends reducing the intake of refined free sugars, which include monosaccharides and disaccharides (e.g., sucrose) added to foods and beverages and sugars naturally present in honey, syrups, fruit juices, and fruit juice concentrate, to less than 10% of the total energy intake (7).

Over the past years, natural sweeteners have sparked much interest as alternatives to refined sugars. Indeed, a

Correspondence: A. Marette (Andre.Marette@criucpq.ulaval.ca).
Submitted 27 February 2023 / Revised 20 September 2023 / Accepted 2 October 2023

0193-1849/23 Copyright © 2023 the American Physiological Society.

Downloaded from journals.physiology.org/journal/ajpendo (061.197.080.176) on January 24, 2025.

growing number of animal studies have shown that natural sugars such as maple syrup (MS) (8, 9), agave syrup (10), and honey (11, 12) have less detrimental effects on glucose homeostasis and/or the lipid profile as compared with an equivalent amount of refined sugars. MS is a minimally transformed sweetener obtained by thermal evaporation of the watery sap collected in late winter and early spring from certain maple (genus *Acer*) species, notably the sugar maple (*Acer saccharum* Marsh), which is native to North America (13). Although the dry content of MS mostly consists of sucrose (97%), our group has nonetheless demonstrated that both acute and chronic administration of MS was less deleterious on glycemic and insulinemic responses in obese rats when compared with animals receiving an equivalent dose of refined sugar (14, 15). In addition, previous animal studies have suggested that an MS extract could exert a positive effect on liver health by modifying the expression of genes related to lipid metabolism (16–20). Taken together, these results indicate that substituting refined sugars with MS could represent a more favorable alternative.

MS contains a variety of macro- and micronutrients such as amino acids, organic acids (succinic and fumaric acid), minerals (potassium, calcium, and magnesium), and vitamins (B2 and niacin). It also contains several polyphenols, including lignans, coumarins, and stilbene (21, 22). The process of boiling the sap to produce MS not only concentrates these phytochemicals but was also reported to generate a new polyphenol named quebecol (23). The presence of polyphenols was shown to inhibit the carbohydrate-hydrolyzing enzyme α-glucosidase in vitro (24). Moreover, it was previously reported that MS contains inulin, a prebiotic fiber specifically fermented by the gut microbiota (25).

In the past 15 years, numerous studies pinpointed functional links between the gut microbiota and host metabolism. As such, an increasing body of evidence reported significant associations between gut microbes, their metabolites, and metabolic disorders such as obesity, type 2 diabetes, and fatty liver diseases (26–28). Hence, the presence of polyphenols, which possess a prebiotic-like activity and decrease carbohydrate digestion, could help reshape the gut microbiota and explain the health benefits provided by substituting sucrose with MS (29, 30). However, to our knowledge, no studies have thoroughly investigated the prebiotic-like action of MS and its impact on metabolic disorders related to obesity such as fatty liver disease and insulin resistance.

This study aimed to investigate whether the metabolic benefits of substituting sucrose with an equivalent dose of MS could be linked to changes in gut microbiota composition and intestinal digestion of carbohydrates in a mouse model of diet-induced obesity.

METHODS

Animals and Diet Treatments

Six-wk-old C57Bl/6J male mice (Jackson, Bar Harbor, ME) were individually housed in a controlled environment (12 h day/night cycle, lights off at 18:00) with food and water ad libitum in the animal facility of the Québec Heart and Lung Institute (Québec City, QC, Canada). After 2 wk of acclimatization on a low-fat diet, mice were assigned to a low-fat low-sucrose diet (LFLS) (10% lipids, 13% proteins, and 78% carbohydrates), a high-fat high-sucrose diet (HFHS) (62.5% of energy from lipids, 14.8% from proteins, and 22.5% from sucrose), or an isocaloric HFHS diet in which a fraction of the sucrose was replaced with MS (62.5% of energy from lipids, 13% from protein, 19% from sucrose, and 3.5% from MS). HFHS-fed mice were also gavaged with sucrose (HFHS + S) ($n = 12$) or MS (HFHS + MS) ($n = 12$) providing 6.5% of their total energy intake. LFLS-fed mice were gavaged with the vehicle (water) (LFLS + V) ($n = 11$) (Table 1). The proportion of calories provided by MS or sucrose by gavage (6.5% of the total energy intake) was determined according to the estimated energy intake provided by added sugar from sugar-sweetened beverages (31), whereas the energy provided from MS or sucrose in the diet (3.5% of the total energy intake) represented the added sugars found in foods. Maple syrup was kindly provided by the Federation of Maple Syrup Producers of Québec and consisted of light, amber, and dark syrups, mixed in equivalent proportions.

Body weight gain and food intake were assessed twice a week. Body composition was analyzed by magnetic resonance at *weeks 0* and *8* (Bruker Minispec LF90II, Bruker Optics, Germany). Fresh feces were collected at *weeks 0* and *8*. At *week 8*, animals were anesthetized in chambers saturated with isoflurane and then euthanized by cardiac puncture. Tissues were harvested and blood was drawn in tubes coated with EDTA and centrifuged. Absence of dermatitis dehydration and weight gain were absolute inclusion criteria for animals. This study followed the Guide for the Care and Use of Laboratory Animals and all procedures had been previously approved by the Laval University Animal Ethics Committee (CPAUL 2018-081-1).

Glucose and Insulin Tolerance

At 5 wk, mice were fasted for 6 h and were subjected to an intraperitoneal insulin tolerance test (ITT) (0.65 U/kg body wt). Blood was collected by the caudal vein and glycemia was measured with an Accu-Check glucometer (Bayer) before (0 min) and after (5, 10, 15, 20, 30, 60 min) intraperitoneal insulin injection. At the end of *week 7*, mice were fasted overnight (12 h) and subjected to an oral glucose tolerance test (OGTT) (1 g of glucose/kg body wt). Blood was collected by the caudal vein before (0 min) and after (15, 30, 60, 90, 120 min) glucose bolus for measuring glycemia and insulinemia measurements. For ITT and GTT, mice were gavaged with vehicle, sucrose, or MS after the test.

Oil-Red O Staining

During the euthanasia, mouse livers were embedded in Tissue-Tek OCT, immediately snap-frozen in liquid nitrogen, and stored at −80°C. Staining of neutral lipids was based on the methods described by Mehlem et al. (32) with some adaptations, as previously described (33). In brief, 12-mm liver sections were allowed to equilibrate at room temperature for 5 min and then postfixed with formalin (10%)/calcium (2%) solution for 15 min. The sections were then incubated with Oil-Red O (ORO) working solution at room temperature for 5 min, followed by a 5-min clearing in 60% isopropyl alcohol and a counterstaining of 15 s with Mayer's hematoxylin. Pictures of liver sections were taken with a wide-field microscope (Zeiss)

Downloaded from journals.physiology.org/journal/ajpendo (061.197.080.176) on January 24, 2025.

Table 1. *Diet composition*

Ingredient	LFLS + V		HFHS + S		HFHS + MS	
	g/100 g	Energy, %	g/100 g	Energy, %	g/100 g	Energy, %
Casein high nitrogen	12.88	12.74	20.48	14.70	20.48	14.70
L-cystine	0.30	0.35	0.17	0.13	0.17	0.13
Sucrose	6.64	7.73	23.17	17.50	23.17	17.50
Starch	62.75	66.43				
Maple syrup					6.90	3.51
Sucrose syrup			6.90	3.51		
Alphacel nonnutritive bulk	5.03		4.66		4.66	
Mineral mix	6.74	0.93	6.24	0.56	6.24	0.56
Vitamin mix	1.41	1.61	1.30	0.97	1.30	0.97
Lard	2.68	7.01	18.43	31.32	18.43	31.32
Corn oil	1.23	3.21	18.43	31.32	18.43	31.32
Choline bitartrate	0.30		0.19		0.19	
Tert-butylhydrytoluene (BHT)	0.03		0.03		0.03	
Total	100	100	100	100	100	100

LFLS + V, low-fat low-sucrose gavaged with vehicle; HFHS + S, high-fat high-sucrose gavaged with sucrose; HFHS + MS, high-fat high-sucrose gavaged with maple syrup (MS).

within 30 min after staining. Quantification of ORO-positive area was done with Image-Pro Plus software. To calculate the mean ORO-positive sections of each mouse, eight pictures of the same liver sections were quantified.

Analytical Methods

Plasma insulin concentration was measured using an ultrasensitive ELISA kit (Alpo, Salem, NH and Chrystal Chem, Elk Grove Village, IL, respectively). Liver triglycerides and cholesterol were extracted with chloroform-methanol. Liver and plasmatic triglyceride and cholesterol content were measured by enzymatic reactions with commercial kits (Randox Laboratories). Cytokines were quantified in 50 μL of liver lysate (100 ng of protein in PBS containing 0.5% bovine serum albumin) using Bio-Plex Pro Assay Moue Cytokine (Bio-Rad). Cytokines below the limit of detection were not considered for analysis. Lipid peroxidation was assessed by thiobarbituric acid reactive substances (TBARSs) assay kit (R&D Systems).

α-Glucosidase Activity Assay

A supplementary group of 8-wk-old chow-fed mice were acclimated for 2 wk in the animal facility. Mice were fasted overnight and gavaged with 2 g/kg of sugar provided either from sucrose syrup ($n = 12$) or from MS ($n = 12$), both containing 0.87 g/mL. Mice were then immediately euthanized, and intestines were collected. A 10-mg section of the ileum was added to 200 μL of ice-cold α-glucosidase assay buffer. Samples were homogenized and supernatant was collected to measure α-glucosidase activity as instructed by the manufacturer (Abcam). In brief, α-glucosidase hydrolyzes the substrate mix to release p-nitrophenol that is measured colorimetrically (optical density = 410 nm). Optical density was measured before (0) and after (60 min) α-glucosidase substrate mix was added.

Cecal Short-Chain Fatty Acid Quantification

Cecum short-chain fatty acid (SCFA) was quantified by gas chromatography. Phosphoric acid was purchased from VWR. Diethyl ether (99.5%) and all the 99% grade standards (acetic acid, propionic acid, isobutyric acid, butyric acid, isovaleric acid, valeric acid, and internal standard 4-methyl valeric acid) were purchased from Sigma-Aldrich. Ceca were collected and kept frozen at −80°C until extraction. After the addition of 1 mL H_2O per 100 mg of material, fecal suspensions were homogenized for 2 min and then centrifuged at 18,000 *g* for 10 min at 4°C. The supernatants were spiked with 4-methylvaleric acid and acidified with phosphoric acid 10%. To extract SCFAs, samples were mixed for 2 min with an equal volume of diethyl ether and then centrifuged at 18,000 *g* for 10 min at 4°C. Organic phase analysis was performed on a gas chromatography with flame ionization detector (GC-FID) system (Shimadzu), consisting of a GC 2010 Plus gas chromatograph equipped with an AOC-20s auto sampler, an AOC-20i auto injector, and a flame ionization detector. The system was controlled by GC solution software. SCFAs were separated on a Nukol capillary GC column [30 m × 0.25 mm inner diameter (ID), 0.25 μM film thickness, Supelco Analytical]. The column flow was constant at 1.3 mL/min of hydrogen. The injector was set at 230°C, and the detector was set at 250°C. The oven temperature was initially programmed at 60°C, then increased to 200°C at 12°C/min, and held for 2 min. SCFA was quantified using a 5-point calibration curve prepared with a mix of acetic acid, propionic acid, butyric acid, isobutyric acid, valeric acid, isovaleric acid, and internal standard 4-methyl valeric acid.

RNA Sequencing Analysis

Livers were collected at euthanasia and were snap-frozen. RNA was extracted from the tissue with the Direct-zol RNA Miniprep Plus (Zymo Research) and sent to Genome Québec (GQ) for sequencing. Analyses of RNA sequences were processed on Galaxy's public server (usegalaxy.org). The quality of FASTQ sequences was assessed with the FASTQC (34) tools (Galaxy Version 0.72) and Illumina adaptors were removed with Cutadapt (35) (Galaxy Version 1.16.6). The resulting sequences were mapped on the mouse reference genome (mm10) with RNA STAR (36) (Galaxy Version 2.7.5b). FeatureCounts (37) tool (Galaxy Version 1.6.4) was used to determine the number of reads per annotated gene. Differential expression analysis between HFHS + S and HFHS + MS mice was performed using DESeq 2 (38) (Galaxy Version 2.11.40.6). The detected genes were considered as

Downloaded from journals.physiology.org/journal/ajpendo (061.197.080.176) on January 24, 2025.

differentially expressed when the false discovery rate (FDR)-adjusted *P* value was under 0.05. Then, functional enrichment analysis was realized on the resulting significant genes using GOseq (39) (Galaxy Version 1.36.0) and the categories selected were Gene Ontology (GO) Cellular Component, GO Biological Process, GO Molecular Function, and Kyoto Encyclopedia of Genes and Genomes (KEGG) pathway. GO terms and KEGG pathways determined were significant when the FDR-adjusted *P* value was under 0.05. Raw RNA-seq data can be accessed through the European Nucleotide Archive (ENA) database with the following accession number: PRJEB66211.

Fecal DNA Extraction

Fecal samples were freshly collected after 8 wk of treatment and immediately stored at −80°C. Bacterial genomic DNA was extracted from ∼50 mg of fecal material collected from each mouse. Samples were homogenized using a bead beater and 0.1-mm zirconium beads and then processed using a DNA extraction kit (Zymo Research, California). DNA yield was assessed using a NanoDrop ND-1000 spectrophotometer (Thermo Scientific). Extracted DNA was stored at −20°C until use.

16S rRNA Gene Amplicon and Shotgun Metagenomic Sequencing

Each DNA sample was subsequently used for 16S amplification of the V3-V4 region using the primers 341 F (5′-CCTACGGGNGGCWGCAG-3′) and 805 R (5′-GACTACHVGGGTATCTAATCC-3′) adapted to incorporate the transposon-based Illumina Nextera adapters (Illumina, California) and a sample barcode sequence allowing multiplexed paired-end sequencing at Institut de Biologie Intégrative et des Systèmes (IBIS, Université Laval). Constructed 16S metagenomic libraries were purified using 35 μL of magnetic beads (AxyPrep Mag PCR Clean-up kit; Axygen Biosciences, New York) per 50μL PCR reaction. Library quality control was performed with a Bioanalyzer 2100 using DNA 7500 chips (Agilent Technologies, California). An equimolar pool was obtained and checked for quality before further processing. The pool was quantified using PicoGreen (Life Technologies, California) and loaded on a MiSeq platform using 2 × 300bp paired-end sequencing (Illumina, California). High-throughput shotgun sequencing was performed at GQ. Two pools of four samples (4 HFHS + S group and 4 HFHS + MS group) were also subjected to shogun sequencing. Metagenomic libraries were prepared using the NEBNext Ultra II DNA Library Prep Kit for Illumina (New England BioLabs) as per the manufacturer's recommendations. Libraries were quantified using the Kapa Illumina GA with Revised Primers-SYBR Fast Universal kit (Kapa Biosystems, Massachusetts). The average size fragment was determined using a LabChip GX (PerkinElmer) instrument. Libraries were sequenced on the Illumina NovaSeq 6000 platform using a 2 × 150 bp paired-end run. This yielded an average number of read pairs per sample of around 32 million.

Amplicon-Based Taxonomic Analysis

Forward and reverse primers were removed from 16S rRNA gene amplicons using Cutadapt (v1.14; 34). Sequence reads were analyzed using the dada2 package (v1.26; 39) in R (http://www.R-project.org). Forward and reverse reads were first trimmed to remove low-quality regions. Dereplication and denoising of filtered sequences were carried out using DADA2 default parameters. Denoised forward and reverse reads were merged (all reads with any mismatches were removed) and searched for chimeras. Taxonomic assignment of amplicon sequence variants (ASVs) was performed using the RDP classifier algorithm (v2.2; 40) trained against the Silva database 138.1 (41). Taxa that appeared less than three times in the entire dataset were removed. Normalization of unequal sample size was performed by rarefying the ASV table at a depth of 8,259 sequences.

Taxonomic and Functional Profiling of Metagenomic Reads

Metagenomic reads were quality-filtered using Trimmomatic with a cutoff ≥Q20 (42) and further filtered to remove the host-origin reads using Bowtie2 (43). Host-decontaminated reads were taxonomically profiled at the species level using SLIMM (44). Taxa with abundance lower than 0.1% and that appeared less than three times in the entire dataset were removed. Functional analysis was completed using HUMAnN2 (45). Subsequently, HUMAnN2 results were grouped into pathways based on the KEGG gene annotation database (46).

Microbiota Analyses

The R Phyloseq package (v1.40.0) (47) was used to perform all diversity analyses. Detection of differentially abundant taxa or pathways between groups was performed with the metagenomics biomarker discovery tool linear discriminant analysis effect size (LEfSe) using a linear discriminant analysis (LDA) score threshold >2.0 (48). Differences between two independent groups were determined using Mann–Whitney's test. Correlations between microbiota components and biological parameters were analyzed using Spearman's test. Benjamini–Hochberg (BH) correction (was used for multiple testing. A *P* value lower than 0.05 was considered statistically significant.

Statistical Analysis

Statistical analysis between HFHS + S- versus HFHS + MS-fed mice was performed using a two-tailed *t* test (GraphPad). LFLS + V-fed mice were only used as a reference group and were therefore not planned in the statistical analyses. Body weight gain, energy intake, glycemia, and insulinemia curves were statistically compared using two-way repeated-measures ANOVA with a Bonferroni post hoc test to assess the impact of time and dietary intervention on the abovementioned parameters (SigmaPlot). All results were considered statistically significant at $P < 0.05$, where * shows the difference between HFHS + S versus HFHS + MS. Data are expressed as means ± SE.

RESULTS

As expected, mice fed LFLS gained considerably less weight than HFHS-fed mice. Total weight gain and energy intake were similar between HFHS + S- and HFHS + MS-fed mice (Fig. 1, *A–C*). Organ weights were not significantly different, but a tendency was observed for gastrocnemius weight to be increased by the MS dietary intervention (Table 2).

Downloaded from journals.physiology.org/journal/ajpendo (061.197.080.176) on January 24, 2025.

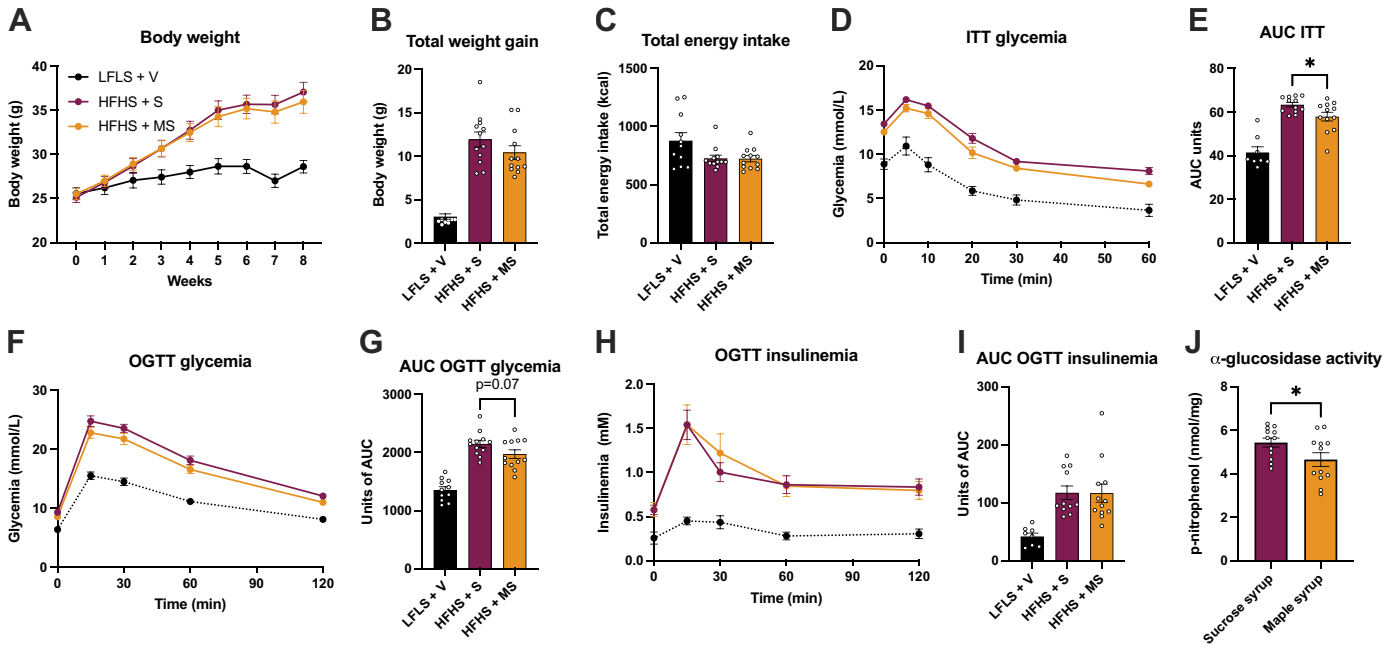

Figure 1. MS does not alter body weight gain but improves glucose homeostasis. Body weight (*A*), total body weight gain (*B*), and total energy intake (*C*). At *week 5*, mice were fasted for 6 h and were subjected to an ITT. Glycemia during ITT (*D*) and area under the curve (AUC) of glycemia during ITT (*E*). At *week 7*, mice were fasted overnight (12 h) and an oral glucose tolerance test (OGTT) was performed. Glycemia during OGTT (*F*), area under the curve (AUC) of glycemia during OGTT (*G*), insulinemia during OGTT (*H*), and AUC of insulinemia during OGTT (*I*). *J*: α-glucosidase activity after 60 min. Data are expressed as means ± SE. *A*, *D*, *F*, and *H*: two-way ANOVA (time × column factor). *B*, *C*, *E*, *F*, *G*, *I*, and *J*: two-tail *t* test to compare HFHS + S to HFHS + MS. *$P < 0.05$ HFHS + S vs. HFHS + MS. Data are expressed as means ± SE ($n = 12$). LFLS + V, fed low-fat low-sucrose and gavaged with the vehicle; HFHS + S, fed high-fat high-sucrose and gavaged with sucrose; HFHS + MS, fed high-fat high-sucrose and gavaged with maple syrup; ITT, insulin tolerance test.

After 5 wk of intervention, mice were fasted for 6 h and were subjected to an ITT (Fig. 1*D*). Insulin tolerance was less deteriorated by MS than sucrose syrup in HFHS-fed mice, as expressed by the decreased area under the curve (AUC) of glycemia (in the HFHS + MS group (Fig. 1*E*). Week 7 into the diet, mice were fasted overnight, and an OGTT was performed (Fig. 1*F*). HFHS-induced glucose intolerance tended to be decreased by MS, as shown by the AUC (Fig. 1*G*). However, no changes in circulating levels of insulin during OGTT were detected (Fig.1, *H* and *I*). Taken together, these data indicate that even at 10% of the total caloric intake, MS is less detrimental to glucose metabolism than refined sugar.

Table 2. *Organ weight*

Organ	LFLS + V	HFHS + S	HFHS + MS	*P* Value
eWAT, g	0.73 ± 0.05	2.46 ± 0.18	2.13 ± 0.19	0.22
rpWAT, g	0.24 ± 0.02	0.87 ± 0.04	0.84 ± 0.07	0.71
mWAT, g	0.30 ± 0.03	0.78 ± 0.08	0.68 ± 0.09	0.43
Total VAT, g	1.17 ± 0.14	4.11 ± 0.30	3.65 ± 0.35	0.32
iWAT, g	0.35 ± 0.02	0.93 ± 0.08	0.84 ± 0.07	0.38
Total WAT, g	1.49 ± 0.18	5.04 ± 0.37	4.48 ± 0.42	0.33
Liver, g	0.96 ± 0.07	1.27 ± 0.04	1.15 ± 0.06	0.12
Gastroc, g	0.27 ± 0.007	0.27 ± 0.004	0.28 ± 0.005	0.07

A two-tailed *t* test was performed to compare HFHS + S with HFHS + MS. Data are represented as means (g) ± SE ($n = 12$). LFLS + V, low-fat low-sucrose gavaged with vehicle; HFHS + S, high-fat high-sucrose gavaged with sucrose; HFHS + MS, high-fat high-sucrose gavaged with maple syrup (MS); WAT, white adipose tissue; eWAT, epididymal WAT; rpWAT, retroperitoneal WAT; mWAT, mesenteric WAT; VAT, visceral adipose tissue (addition of eWAT, rpWAT, and mWAT); iWAT, inguinal WAT; gastroc, gastrocnemius muscle adjusted for body weight.

To better understand the effects of MS on glucose metabolism, we then measured the α-glucosidase activity, an enzyme located in the intestinal brush border involved in disaccharide digestion to absorbable monosaccharides. For this analysis, another set of mice was administered either a single bolus of MS ($n = 12$) or sucrose ($n = 12$) (2 g/kg) and were euthanized 30 min later. The ileum was immediately collected and enzymatic activity was measured. Administration of MS significantly decreased α-glucosidase activity, suggesting that disaccharides were less digested, and thus less absorbed (Fig. 1*J*). In the long-term study, as MS was administered daily by both gavage and in food, this may have prevented sugar absorption to a certain extent and partly protected from chronic hyperglycemia and glucose homeostasis deterioration.

We then investigated the impact of replacing 10% of the total caloric intake by MS in HFHS-fed mice on hepatic health. Although MS did not alter liver weight (Fig. 2*A*), the treatment decreased liver steatosis in HFHS-fed animals, as shown by reduced hepatic triglyceride levels (Fig. 2*B*). Hepatic cholesterol levels and ORO-positive area were not significantly reduced by MS (Fig. 2, *C* and *D*). To explore the potential impact of MS on liver inflammation, a multiplex assay was performed. No changes in inflammatory markers such as interleukin-6 (IL-6), monocyte chemoattractant protein-1 (MCP-1), tumor necrosis factor-alpha (TNF-α), and interleukin-10 (IL-10) levels were observed between HFHS-fed mice (Supplemental Fig. S1, *A*–*D*). In line with this, no changes in lipid peroxidation, as evidenced by thiobarbituric acid reactive substances (TBARSs), were detected in liver homogenates (Supplemental Fig. S1*E*) (all supplemental material is available at https://doi.org/10.6084/m9.figshare.22149206.v1).

Downloaded from journals.physiology.org/journal/ajpendo (061.197.080.176) on January 24, 2025.

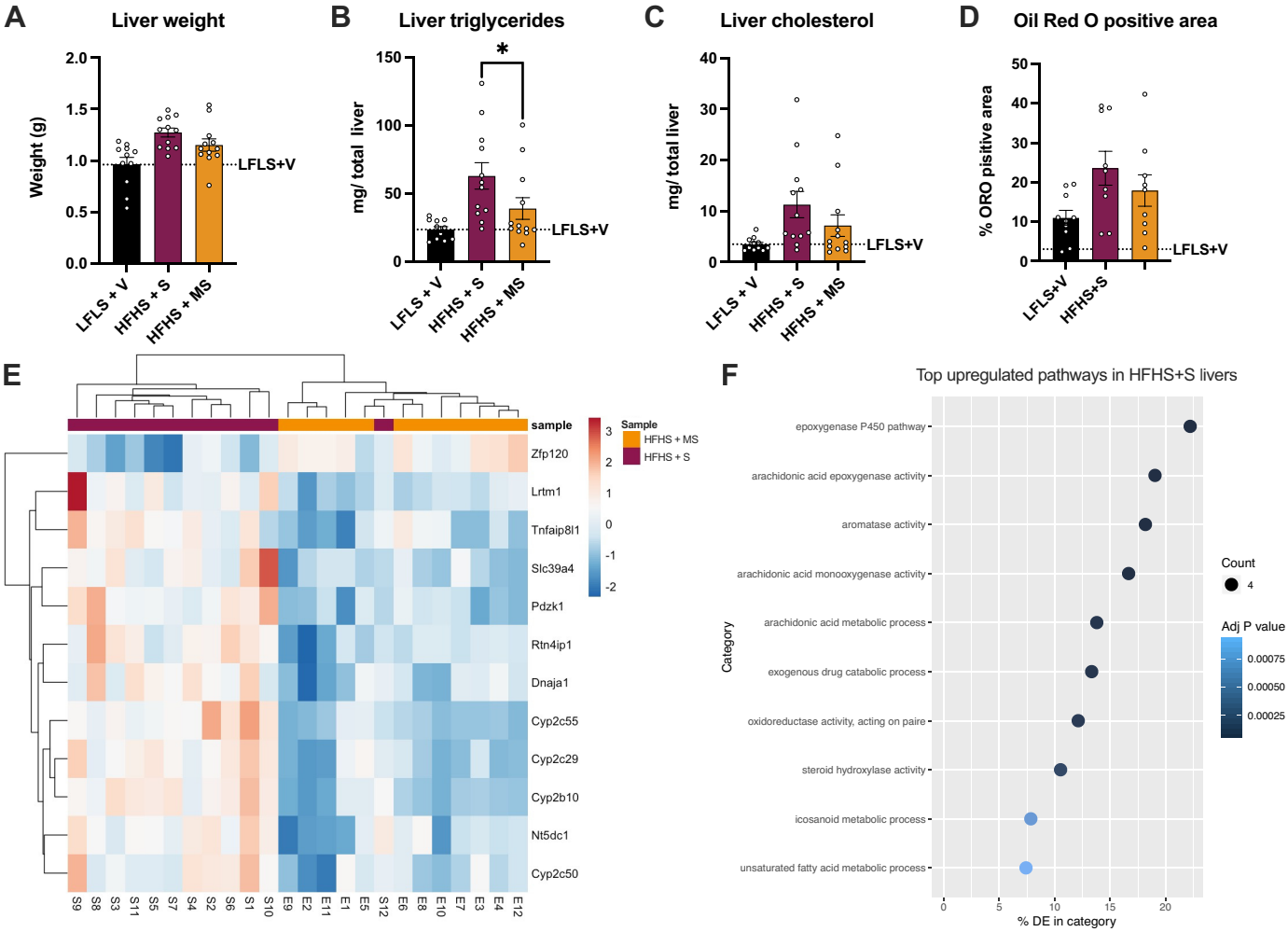

Figure 2. Maple syrup decreases liver triglyceride accumulation and alters gene expression related to anti-inflammatory defense. *A*: liver weight. Liver triglycerides (*B*) and cholesterol (*C*) were measured from liver homogenates. *D*: quantification of oil-red O (ORO)-positive area. *E*: hierarchical clustering analysis of liver genes. The heatmap illustrates *z*-scores of differentially expressed genes between HFHS + S- and HFHS + MS-fed mice. Different columns represent different samples, and different rows represent different genes. Red corresponds to genes that are significantly upregulated, and blue corresponds to those that are significantly downregulated. *F*: the top 10 overrepresented GO terms in HFHS + S ranked in *P* values. Data are expressed as means ± SE. A two-tailed *t* test was performed to compare HFHS + S with HFHS + MS. *$P < 0.05$ HFHS + S vs. HFHS + MS. Data are expressed as means ± SE ($n = 12$). DE, differentially expressed; GO, Gene Ontology; HFHS + S, fed high-fat high-sucrose and gavaged with sucrose; HFHS + MS, fed high-fat high-sucrose and gavaged with maple syrup.

To further analyze the impact of MS on hepatic health, a transcriptomic analysis was performed. Clustering of HFHS + S and HFHS + MS gene expression revealed significant differences between the two HFHS-fed groups (Fig. 2*E*). Only one gene, zinc finger protein 120 (*Zfp120*) was significantly overrepresented in the livers of HFHS + MS-fed mice. On the other hand, several genes were upregulated in the livers of HFHS + S-fed mice. Most of these genes (e.g., *Cyp2c55*, *Cyp2c29*, *Cyp2b10*, and *Cyp2c50*) encode for proteins involved in the cytochrome P450 (Cyp450) epoxygenase pathway of arachidonic acid (AA) metabolism, which generates arachidonic acid epoxides, also known as epoxyeicosatrienoic acids (EETs). In line with this, KEGG analysis highlighted that the most upregulated pathways in the livers of HFHS + S-fed mice compared with HFHS + MS-fed mice were related to the arachidonic acid epoxygenase activity (Fig. 2*F*). EETs are known as anti-inflammatory mediators (40). Differentially expressed genes related to the epoxygenase pathway in the livers of HFHS + S-fed mice could suggest an early response to counter inflammatory stimulus induced by steatosis. This could lead to lower cytokine levels, which were brought to a similar level as those of HFHS + MS-fed mice, who were protected from steatosis.

As MS contains a diversity of bioactive compounds such as polyphenols and inulin, which are both specifically metabolized by the gut microbiota, we next investigated its impact on fecal microbiota by 16S rRNA sequencing (Supplemental Fig. S2) and whole genome shotgun sequencing (Fig. 3*A*). The bacterial composition of the two HFHS-fed groups clustered differently, as evidenced by the principal coordinate analysis (Fig. 3*D*). Linear discriminant analysis (LDA) effect size (LEfSe) analysis revealed that the feces of HFHS + MS-fed mice harbored significantly more *Faecalibaculum rodentium*, *Romboutsia ilealis*, and *Lactobacillus johnsonii* (Fig. 3*B*). Shotgun sequencing also revealed that bacterial metabolic pathways were altered between both HFHS-fed groups. On one hand, pathways related to the pentose and glucuronate

Downloaded from journals.physiology.org/journal/ajpendo (061.197.080.176) on January 24, 2025.

interconversions, phenylalanine tyrosine and tryptophan biosynthesis, riboflavin metabolism, and valine leucine and isoleucine biosynthesis were upregulated in the microbiome of HFHS + S-fed mice. On the other hand, MS increased pathways related to primary and secondary bile acids, phosphotransferase system (PTS), pyrimidine metabolism, nucleotide excision repair, and alanine metabolism (Fig. 3*C*).

As *F. rodentium* is a known butyrate producer, we next investigated the cecal short-chain fatty acid profile. Butyric acid levels tended ($P = 0.09$) to be higher in the cecum of HFHS + MS-fed mice (Fig. 3*G*), whereas isovalerate was significantly increased by MS (Fig. 3*H*). No changes in acetic, propionic, valeric, and isobutyric acid were detected (Fig. 3, *E*, *F*, *I*, and *J*).

DISCUSSION

Our work shows that substituting sucrose with an isocaloric portion of MS, representing only 10% of the total energy intake in an obesogenic diet, alleviated insulin resistance and reduced liver triglyceride accumulation in an 8-wk intervention. This could partly be explained by decreased carbohydrate digestion and absorption, as evidenced by lower intestinal α-glucosidase activity in HFHS + MS-fed mice. Moreover, transcriptomic analysis revealed that the Cyp450 epoxygenase pathway of arachidonic acid metabolism was significantly upregulated in the livers of HFHS + S-fed mice as compared with mice administered MS. Apart from its sucrose composition, complexity of the MS

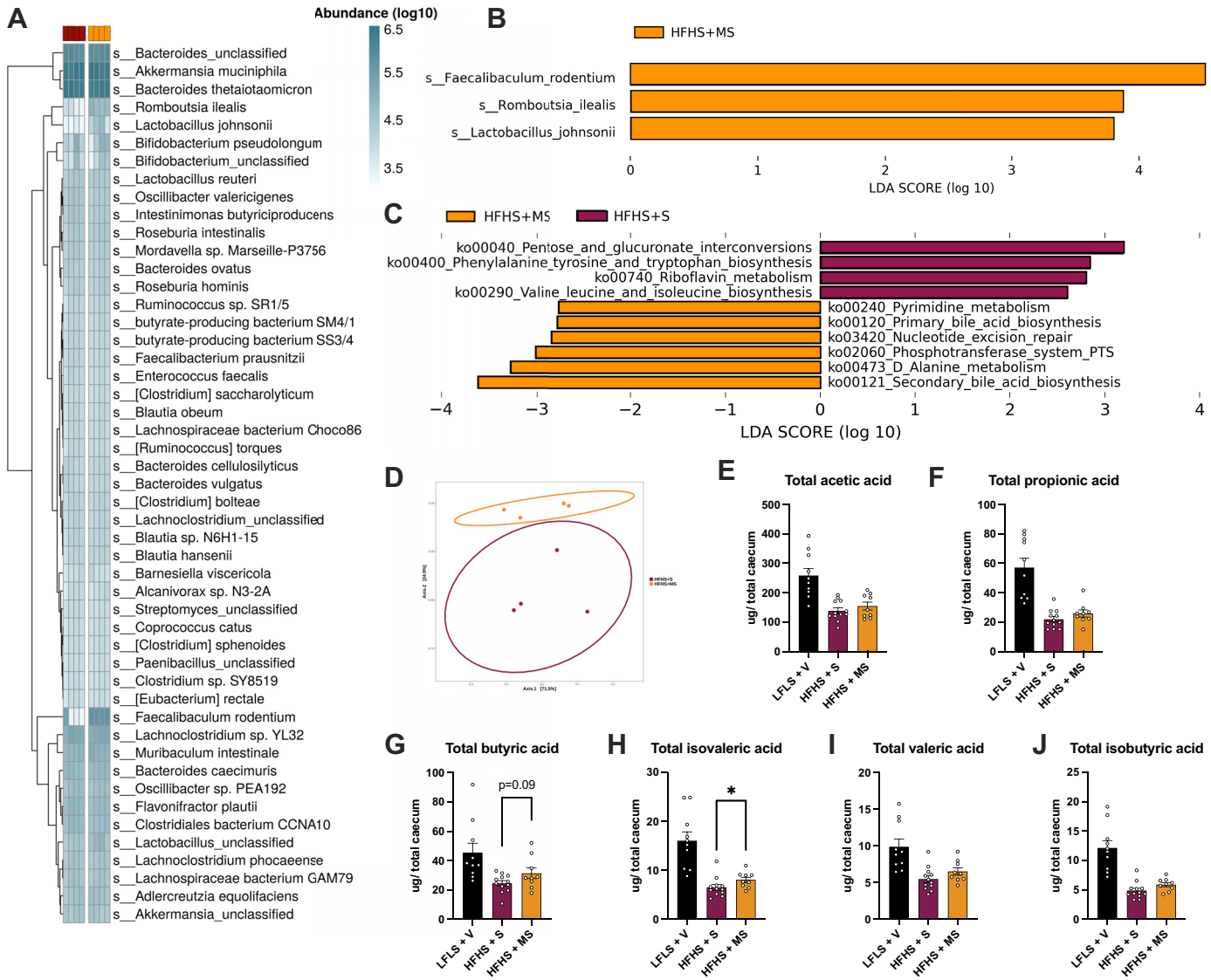

Figure 3. Fecal microbiota and microbiome changes following the dietary intervention. Fecal samples were collected on the 8th wk. *A*: heatmap of bacterial species abundance after 8 wk of dietary intervention. *B*: linear discriminant analysis (LDA) effect size (LefSe) was calculated to explore the taxa that most strongly discriminate between the gut microbiota of mice fed HFHS + S and HFHS + MS. *C*: LefSe was also calculated to explore the significantly different pathway abundance between HFHS + S and HFHS + MS. *D*: principal coordinates analysis (PCoA) based on Bray–Curtis dissimilarity matrix. Cecal content was used to measure acetic acid (*E*), propionic acid (*F*), butyric acid (*G*), isovaleric acid (*H*), valeric acid (*I*), and isobutyric acid (*J*). *E*–*J*: two-tail *t* test to compare HFHS + S- with HFHS + MS-fed mice. *$P < 0.05$ HFHS + S vs. HFHS + MS. Data are expressed as means ± SE ($n = 12$). HFHS + S, fed high-fat high-sucrose and gavaged with sucrose; HFHS + MS, fed high-fat high-sucrose and gavaged with maple syrup.

Downloaded from journals.physiology.org/journal/ajpendo (061.197.080.176) on January 24, 2025.

composition also induced significant changes in gut microbiota composition, as evidenced by an increased abundance of *F. rodentium*, *R. ilealis*, and *L. johnsonii* in the feces of HFHS + MS-fed mice. Although metabolic pathways in the microbiome of HFHS + S-fed mice were mostly involved in proteolytic fermentation, MS increased metabolic pathways and the abundance of bacteria involved in carbohydrate metabolism. Notably, the phosphotransferase system (PTS) was increased in the microbiome of HFHS + MS-fed mice, which could contribute to the increased bioavailability of polyphenols.

In line with other studies investigating the long-term impact of substituting sucrose with MS in rats (9, 14), no changes in the body weight of HFHS + MS-fed mice were detected. This was also reported in KK-A^{y} mice fed a diet containing 0.1% polyphenol-rich MS extract (18). Despite the absence of changes in body weight, mice administered MS had decreased glycemia during ITT and tended to have improved glycemia during OGTT. In a previous study performed by our group, the composition of MS was analyzed and revealed that it contains several bioactive molecules, such as polyphenols and phytohormones. Indeed, MS contains high levels of abscisic acid (ABA) and phaseic acid (PA), a metabolite of ABA (22). The occurrence of these phytohormones in MS is of interest considering that they have been studied for their efficacy in the treatment of diabetes and inflammation (41, 42). Moreover, it was previously reported that MS can inhibit the activity of α-glucosidase, an enzyme located in the brush border of the small intestine involved in disaccharide digestion, consequently releasing absorbable monosaccharides (glucose, fructose, and galactose), although this effect was only observed in vitro (24, 43). We thus propose that daily substitution of refined sucrose by MS for 8 wk generated lower glycemic and insulinemic responses, translating to a less deteriorated glucose homeostasis as compared with refined sugar consumption.

We also observed that mice administered MS accumulated significantly fewer liver triglycerides than mice administered sucrose. To the best of our knowledge, we are the first to report this finding. Indeed, although other studies investigated the impact of a polyphenolic-rich maple syrup extract (MSX) on hepatic health in obese C57Bl/6J mice, no significant differences were observed in the hepatic triglyceride content (16, 17). Liver transcriptomic analysis revealed that several cytochrome P450 (CYP) genes were upregulated in the livers of HFHS + S-fed mice compared with HFHS + MS-fed mice and that pathways related to the arachidonic acid epoxygenase activity were upregulated. Arachidonic acid breakdown and metabolism play a major role in triggering and resolving inflammation. Indeed, the balance between anti-inflammatory (epoxyeicosatrienoic acid; EET) and proinflammatory (leukotrienes) metabolites is crucial in many pathophysiological conditions (44). Upon a proinflammatory stimulus, arachidonic acid (AA) stored in phospholipid membranes is hydrolyzed by the cytosolic phospholipase A2 (cPLA2) and is oxidized by CYP2J and CYP2C subfamilies to become anti-inflammatory epoxyeicosatrienoic acids (EETs) (45, 46). Therefore, the activation of the epoxygenase P450 pathway in the livers of HFHS + S-fed mice may be a first line of defense against a proinflammatory insult and, thus, an attempt to limit further damage. On the other hand, those pathways were downregulated in the livers of HFHS + MS-fed mice, suggesting a lower inflammatory tone. This finding is in line with previous studies reporting that both MSX and MS mitigated hepatic inflammation caused by an obesogenic diet (14, 16).

Several studies have now convincingly demonstrated that the gut microbiota plays a central role in metabolic health through a variety of mechanisms (47–49). The gut and liver are intrinsically connected and strongly depend on each other in terms of metabolic functioning. Not surprisingly, disturbances in the gut-liver axis, including increased gut permeability and dysbiosis, are linked to non-alcoholic fatty liver disease (NAFLD) (50). Prebiotics are defined as carbohydrates specifically degraded by the gut microbiota, thereby yielding important metabolites, such as SCFA, which are associated with improved metabolic outcomes (50–52). It was previously reported that MS contains inulin, a prebiotic fiber (25). In addition, we and others have reported that MS is a source of lignans, a specific class of polyphenols known for their prebiotic-like action (15, 21, 22). Like many other polyphenols, the bioactivity of lignans depends on their transformation by gut bacteria, as they must undergo deglycosylation by the gut microbiota into enterolignans before entering the organism to exert their positive effect on metabolic health (53, 54). To this day, no studies have reported a significant impact of MS on gut microbiota composition. Therefore, we aimed to thoroughly investigate the impact of substituting refined sugars by MS on gut microbiome by whole genome shotgun sequencing.

Shotgun sequencing revealed that replacing sucrose syrup with an isocaloric amount of MS for 8 wk significantly increased the abundance of *F. rodentium*, *R. ilealis*, and *L. johnsonii*. Interestingly, *Lactobacillus* and *Romboutsia* bacterial families are known to possess genes encoding for the phosphotransferase system (PTS), a bacterial metabolic pathway involved in the utilization of a wide array of simple carbohydrates, such as sucrose, as an energy source (55, 56). Accordingly, we observed that the pathway related to PTS was significantly increased in the microbiome of HFHS + MS-fed mice. In line with the decreased α-glucosidase activity following MS administration, a higher proportion of unabsorbed sugars may be present in the gut lumen and could be used as an energy source through PTS. A recent article also reported that *Lactobacilli* can metabolize the sugar moiety of glycosylated phytochemical compounds and externalize their bioactive aglycone, making them more bioavailable (56). Therefore, the increased PTS pathway may also have contributed to the deglycosylation of polyphenols naturally found in MS and increased their bioavailability.

The metagenomic data revealed that *F. rodentium*, an important butyric acid producer, and *R. ilealis*, a known SCFA producer, were more abundant in the feces of HFHS + MS-fed mice (55, 57). It was previously reported that feeding a symbiotic (a mix of prebiotics and probiotics) to diet-induced obese mice alleviated metabolic disturbances and increased the proportion of *F. rodentium*, which was in turn associated with normalization of the SCFA (58). In line with this, the concentration of butyric acid tended to be increased in the cecum of HFHS + MS-fed mice. In a previous study, the administration of butyric acid to high-fat-fed mice improved the intestinal barrier and attenuated steatohepatitis (59). Apart from being the preferred

Downloaded from journals.physiology.org/journal/ajpendo (061.197.080.176) on January 24, 2025.

fuel for colonocytes, butyric acid is also a major regulator of cell proliferation and differentiation, therefore playing a major role in gut permeability (60). Interestingly, once absorbed in the systemic circulation, SCFA can also exert a hepatoprotective action via a peroxisome proliferator-activated receptor γ (PPARγ)-dependent switch from lipogenesis to fat oxidation in the liver and adipose tissue (61). In line with this, rodent experiments with isotopically labeled SCFAs demonstrated that absorption of SCFA, and not the cecal concentration of SCFA, is relevant for metabolic health. This could therefore explain why we see an improvement in metabolic parameters without observing significant changes in acetate, propionate, and butyrate. Overall, the prebiotic action of MS may have promoted microbiome pathways related to carbohydrate utilization and SCFA production, which were associated with improved metabolic outcomes. As opposed to the microbiome of HFHS + MS-fed mice, the metagenomic analysis revealed that metabolic pathways related to branched-chain amino acids valine, leucine, and isoleucine and to aromatic amino acids phenylalanine, tyrosine, and tryptophan were upregulated in the feces of HFHS + S-fed mice. The proteolytic fermentation yields mainly harmful derivates, such as ammonia and phenol, which might be detrimental to the host gut and metabolic health (50).

This study has major strengths, like a carefully designed diet to mimic the carbohydrate intake from sugar-sweetened beverages, providing 6.5% of the total energy intake (31), and sugar incorporated into the diet. The impact of replacing sucrose with MS was also carefully investigated, notably by analyzing the gut microbiota composition by whole-genome shotgun sequencing and by investigating the mechanistic impact of MS on intestinal carbohydrate digestion. However, this study also contains some limitations. First of all, the study was only conducted in male mice, and the impact of replacing sucrose with MS needs to be further investigated in female mice. In addition, the metabolic improvement observed after 8 wk is small, but this may be explained by the fact that we have used an isocaloric dietary intervention with a small dose of MS, substituting only 10% of the total caloric intake provided by sucrose. This was chosen to remain clinically relevant since such substitutions remain within the range of sugar replacement that is achievable in humans. We believe that if all the sucrose had been replaced by MS, we could have observed a more significant impact on metabolic health. Finally, maple syrup is a natural product and its phytonutrient composition can vary according to the season and the syrup category. In this study, we used a mix of three different types of MS (extra clear, amber, and dark) to account for this variability, but the impact of each MS category should also be further investigated.

In conclusion, the replacement of sucrose by MS in HFHS-fed mice was found to decrease carbohydrate digestion and was less deleterious on metabolic outcomes such as insulin resistance and liver steatosis, in association with changes in the composition of the gut microbiota. The microbiome of MS-treated HFHS-fed animals was reshaped to increase the abundance of bacteria capable of metabolizing polyphenols and carbohydrates, thus producing bioactive metabolites such as butyric acid associated with improved hepatic health. Taken together, these results indicate that substituting refined sugars with MS could represent a more favorable alternative for metabolic health.

DATA AVAILABILITY

Data will be made available upon reasonable request.

SUPPLEMENTAL DATA

Supplemental Figs. S1 and S2: https://doi.org/10.6084/m9.figshare.22149206.v1.

ACKNOWLEDGMENTS

We are grateful to C. Dallaire, J. Dupont-Morissette, J. Julien, and J. Rancourt-Mercier (Québec Heart and Lung Institute, Laval University, Quebec City, QC, Canada) for expert assistance with animal experiments and to P. Feutry (Institute of Nutrition and Functional Foods, Laval University, Quebec City, QC, Canada) for technical support with gas chromatography with flame ionization detector (GC-FID) analysis. Graphical abstract created with BioRender and published with permission.

GRANTS

This study was funded by the Producteurs et productrices acéricoles du Québec (PPAQ). A. Marette was supported by the Canadian Institutes of Health Research/Pfizer-partnered research chair and the J.A. DeSève Foundation.

DISCLAIMERS

This study was funded by the PPAQ, but had no role in data integration, interpretation, and conclusion.

DISCLOSURES

A. Morissette and A. Marette received scholarship and grants from the PPAQ but are neither consultant nor have any commercial interest. None of the other authors has any conflicts of interest, financial or otherwise, to disclose.

Andre Marette is an editor of *American Journal of Physiology-Endocrinology and Metabolism* and was not involved and did not have access to information regarding the peer-review process or final disposition of this article. An alternate editor oversaw the peer-review and decision-making process for this article.

AUTHOR CONTRIBUTIONS

G.P., V.P.H., and A. Marette conceived and designed research; A. Morissette, A.-L.A., T.V.V., and N.F. performed experiments; A. Morissette and A.-L.A. analyzed data; A. Morissette and A.-L.A. interpreted results of experiments; A. Morissette prepared figures; A. Morissette drafted manuscript; A. Morissette, A.-L.A., T.V.V., G.P., N.F., V.P.H., and A. Marette edited and revised manuscript; A. Morissette, D.M.A., A.-L.A., T.V.V., G.P., N.F., V.P.H., and A. Marette approved final version of manuscript.

REFERENCES

1. **Blüher M.** Obesity: global epidemiology and pathogenesis. *Nat Rev Endocrinol* 15: 288–298, 2019. doi:10.1038/s41574-019-0176-8.
2. **World Obesity.** World Obesity Atlas 2022. https://www.worldobesity.org/resources/resource-library/world-obesity-atlas-2022.
3. **World Health Organization.** Obesity and Overweight. https://www.who.int/en/news-room/fact-sheets/detail/obesity-and-overweight.
4. **Malik VS**, **Hu FB.** The role of sugar-sweetened beverages in the global epidemics of obesity and chronic diseases. *Nat Rev Endocrinol* 18: 205–218, 2022. doi:10.1038/s41574-021-00627-6.
5. **Bray GA**, **Popkin BM.** Dietary sugar and body weight: have we reached a crisis in the epidemic of obesity and diabetes?: health be

Downloaded from journals.physiology.org/journal/ajpendo (061.197.080.176) on January 24, 2025.

damned! Pour on the sugar. *Diabetes Care* 37: 950–956, 2014. doi:10.2337/dc13-2085.
6. **Lustig RH**, **Schmidt LA**, **Brindis CD.** Public health: the toxic truth about sugar. *Nature* 482: 27–29, 2012. doi:10.1038/482027a.
7. **World Health Organization**. WHO Calls on Countries to Reduce Sugars Intake among Adults and Children. https://www.who.int/mediacentre/news/releases/2015/sugar-guideline/en/.
8. **Nagai N**, **Ito Y**, **Taga A.** Comparison of the enhancement of plasma glucose levels in type 2 diabetes Otsuka Long-Evans Tokushima Fatty rats by oral administration of sucrose or maple syrup. *J Oleo Sci* 62: 737–743, 2013. doi:10.5650/jos.62.737.
9. **Nagai N**, **Yamamoto T**, **Tanabe W**, **Ito Y**, **Kurabuchi S**, **Mitamura K**, **Taga A.** Changes in plasma glucose in Otsuka Long-Evans Tokushima Fatty rats after oral administration of maple syrup. *J Oleo Sci* 64: 331–335, 2015. doi:10.5650/jos.ess14075.
10. **Hooshmand S**, **Holloway B**, **Nemoseck T**, **Cole S**, **Petrisko Y**, **Hong MY**, **Kern M.** Effects of agave nectar versus sucrose on weight gain, adiposity, blood glucose, insulin, and lipid responses in mice. *J Med Food* 17: 1017–1021, 2014. doi:10.1089/jmf.2013.0162.
11. **Al-Waili NS.** Natural honey lowers plasma glucose, C-reactive protein, homocysteine, and blood lipids in healthy, diabetic, and hyperlipidemic subjects: comparison with dextrose and sucrose. *J Med Food* 7: 100–107, 2004. doi:10.1089/109662004322984789.
12. **Yaghoobi N**, **Al-Waili N**, **Ghayour-Mobarhan M**, **Parizadeh SM**, **Abasalti Z**, **Yaghoobi Z**, **Yaghoobi F**, **Esmaeili H**, **Kazemi-Bajestani SM**, **Aghasizadeh R**, **Saloom KY**, **Ferns GA.** Natural honey and cardiovascular risk factors; effects on blood glucose, cholesterol, triacylglycerole, CRP, and body weight compared with sucrose. *ScientificWorldJournal* 8: 463–469, 2008. doi:10.1100/tsw.2008.64.
13. **Ball DW.** The chemical composition of maple syrup. *J Chem Educ* 84: 1647, 2007. doi:10.1021/ed084p1647.
14. **Valle M**, **St-Pierre P**, **Pilon G**, **Marette A.** Differential effects of chronic ingestion of refined sugars versus natural sweeteners on insulin resistance and hepatic steatosis in a rat model of diet-induced obesity. *Nutrients* 12: 2292, 2020. doi:10.3390/nu12082292.
15. **St-Pierre P**, **Pilon G**, **Dumais V**, **Dion C**, **Dubois M-J**, **Dubé P**, **Desjardins Y**, **Marette A.** Comparative analysis of maple syrup to other natural sweeteners and evaluation of their metabolic responses in healthy rats. *J Funct Foods* 11: 460–471, 2014. doi:10.1016/j.jff.2014.10.001.
16. **Kamei A**, **Watanabe Y**, **Shinozaki F**, **Yasuoka A**, **Kondo T**, **Ishijima T**, **Toyoda T**, **Arai S**, **Abe K.** Administration of a maple syrup extract to mitigate their hepatic inflammation induced by a high-fat diet: a transcriptome analysis. *Biosci Biotechnol Biochem* 79: 1893–1897, 2015. doi:10.1080/09168451.2015.1042833.
17. **Kamei A**, **Watanabe Y**, **Shinozaki F**, **Yasuoka A**, **Shimada K**, **Kondo K**, **Ishijima T**, **Toyoda T**, **Arai S**, **Kondo T**, **Abe K.** Quantitative deviating effects of maple syrup extract supplementation on the hepatic gene expression of mice fed a high-fat diet. *Mol Nutr Food Res* 61, 2017. doi:10.1002/mnfr.201600477.
18. **Toyoda T**, **Iida K**, **Ishijima T**, **Abe K**, **Okada S**, **Nakai Y.** A maple syrup extract alleviates liver injury in type 2 diabetic model mice. *Nutr Res* 73: 97–101, 2020. doi:10.1016/j.nutres.2019.10.006.
19. **Toyoda T**, **Kamei A**, **Ishijima T**, **Abe K**, **Okada S.** A maple syrup extract alters lipid metabolism in obese type 2 diabetic model mice. *Nutr Metab (Lond)* 16: 84, 2019. doi:10.1186/s12986-019-0403-2.
20. **Watanabe Y**, **Kamei A**, **Shinozaki F**, **Ishijima T**, **Iida K**, **Nakai Y**, **Arai S**, **Abe K.** Ingested maple syrup evokes a possible liver-protecting effect-physiologic and genomic investigations with rats. *Biosci Biotechnol Biochem* 75: 2408–2410, 2011. doi:10.1271/bbb.110532.
21. **Li L**, **Seeram NP.** Maple syrup phytochemicals include lignans, coumarins, a stilbene, and other previously unreported antioxidant phenolic compounds. *J Agric Food Chem* 58: 11673–11679, 2010. doi:10.1021/jf1033398.
22. **Li L**, **Seeram NP.** Further investigation into maple syrup yields 3 new lignans, a new phenylpropanoid, and 26 other phytochemicals. *J Agric Food Chem* 59: 7708–7716, 2011. doi:10.1021/jf2011613.
23. **Li L**, **Seeram NP.** Quebecol, a novel phenolic compound isolated from Canadian maple syrup. *J Funct Foods* 3: 125–128, 2011. doi:10.1016/j.jff.2011.02.004.
24. **Apostolidis E**, **Li L**, **Lee C**, **Seeram NP.** In vitro evaluation of phenolic-enriched maple syrup extracts for inhibition of carbohydrate hydrolyzing enzymes relevant to type 2 diabetes management. *J Funct Foods* 3: 100–106, 2011. doi:10.1016/j.jff.2011.03.003.
25. **Sun J**, **Ma H**, **Seeram NP**, **Rowley DC.** Detection of inulin, a prebiotic polysaccharide, in maple syrup. *J Agric Food Chem* 64: 7142–7147, 2016. doi:10.1021/acs.jafc.6b03139.
26. **Rastelli M**, **Knauf C**, **Cani PD.** Gut microbes and health: a focus on the mechanisms linking microbes, obesity, and related disorders. *Obesity (Silver Spring)* 26: 792–800, 2018. doi:10.1002/oby.22175.
27. **Ridaura VK**, **Faith JJ**, **Rey FE**, **Cheng J**, **Duncan AE**, **Kau AL**, **Griffin NW**, **Lombard V**, **Henrissat B**, **Bain JR**, **Muehlbauer MJ**, **Ilkayeva O**, **Semenkovich CF**, **Funai K**, **Hayashi DK**, **Lyle BJ**, **Martini MC**, **Ursell LK**, **Clemente JC**, **Van Treuren W**, **Walters WA**, **Knight R**, **Newgard CB**, **Heath AC**, **Gordon JI.** Gut microbiota from twins discordant for obesity modulate metabolism in mice. *Science* 341: 1241214, 2013. doi:10.1126/science.1241214.
28. **Le Roy T**, **Llopis M**, **Lepage P**, **Bruneau A**, **Rabot S**, **Bevilacqua C**, **Martin P**, **Philippe C**, **Walker F**, **Bado A**, **Perlemuter G**, **Cassard-Doulcier AM**, **Gérard P.** Intestinal microbiota determines development of non-alcoholic fatty liver disease in mice. *Gut* 62: 1787–1794, 2013. doi:10.1136/gutjnl-2012-303816.
29. **Zhernakova A**, **Kurilshikov A**, **Bonder MJ**, **Tigchelaar EF**, **Schirmer M**, **Vatanen T**, **Mujagic Z**, **Vila AV**, **Falony G**, **Vieira-Silva S**, **Wang J**, **Imhann F**, **Brandsma E**, **Jankipersadsing SA**, **Joossens M**, **Cenit MC**, **Deelen P**, **Swertz MA**; **LifeLines cohort study**; **Weersma RK**, **Feskens EJ**, **Netea MG**, **Gevers D**, **Jonkers D**, **Franke L**, **Aulchenko YS**, **Huttenhower C**, **Raes J**, **Hofker MH**, **Xavier RJ**, **Wijmenga C**, **Fu J.** Population-based metagenomics analysis reveals markers for gut microbiome composition and diversity. *Science* 352: 565–569, 2016. doi:10.1126/science.aad3369.
30. **Dahiya DK**, **Renuka** , **Puniya M**, **Shandilya UK**, **Dhewa T**, **Kumar N**, **Kumar S**, **Puniya AK**, **Shukla P.** Gut microbiota modulation and its relationship with obesity using prebiotic fibers and probiotics: a review. *Front Microbiol* 8: 563, 2017. doi:10.3389/fmicb.2017.00563.
31. **Rosinger A**, **Herrick K**, **Gahche J**, **Park S.** Sugar-sweetened beverage consumption among U.S. adults, 2011–2014. *NCHS Data Brief* 1–8, 2017.
32. **Mehlem A**, **Hagberg CE**, **Muhl L**, **Eriksson U**, **Falkevall A.** Imaging of neutral lipids by oil red O for analyzing the metabolic status in health and disease. *Nat Protoc* 8: 1149–1154, 2013. doi:10.1038/nprot.2013.055.
33. **Anhê FF**, **Nachbar RT**, **Varin TV**, **Vilela V**, **Dudonné S**, **Pilon G**, **Fournier M**, **Lecours MA**, **Desjardins Y**, **Roy D**, **Levy E**, **Marette A.** A polyphenol-rich cranberry extract reverses insulin resistance and hepatic steatosis independently of body weight loss. *Mol Metab* 6: 1563–1573, 2017. doi:10.1016/j.molmet.2017.10.003.
34. **Andrews S.** FastQC: A Quality Control Tool for High Throughput Sequence Data. http://www.bioinformatics.babraham.ac.uk/projects/fastqc/.
35. **Martin M.** Cutadapt removes adapter sequences from high-throughput sequencing reads. *EMBnet J* 17, 2011. doi:10.14806/ej.17.1.200.
36. **Dobin A**, **Davis CA**, **Schlesinger F**, **Drenkow J**, **Zaleski C**, **Jha S**, **Batut P**, **Chaisson M**, **Gingeras TR.** STAR: ultrafast universal RNA-seq aligner. *Bioinformatics* 29: 15–21, 2013. doi:10.1093/bioinformatics/bts635.
37. **Liao Y**, **Smyth GK**, **Shi W.** featureCounts: an efficient general purpose program for assigning sequence reads to genomic features. *Bioinformatics* 30: 923–930, 2014. doi:10.1093/bioinformatics/btt656.
38. **Love MI**, **Huber W**, **Anders S.** Moderated estimation of fold change and dispersion for RNA-seq data with DESeq2. *Genome Biol* 15: 550, 2014. doi:10.1186/s13059-014-0550-8.
39. **Young MD**, **Wakefield MJ**, **Smyth GK**, **Oshlack A.** Gene ontology analysis for RNA-seq: accounting for selection bias. *Genome Biol* 11: R14, 2010. doi:10.1186/gb-2010-11-2-r14.
40. **Shi Z**, **He Z**, **Wang DW.** CYP450 epoxygenase metabolites, epoxyeicosatrienoic acids, as novel anti-inflammatory mediators. *Molecules* 27: 3873, 2022. doi:10.3390/molecules27123873.
41. **Guri AJ**, **Hontecillas R**, **Si H**, **Liu D**, **Bassaganya-Riera J.** Dietary abscisic acid ameliorates glucose tolerance and obesity-related inflammation in db/db mice fed high-fat diets. *Clin Nutr* 26: 107–116, 2007. doi:10.1016/j.clnu.2006.07.008.
42. **Atkinson FS**, **Villar A**, **Mula A**, **Zangara A**, **Risco E**, **Smidt CR**, **Hontecillas R**, **Leber A**, **Bassaganya-Riera J.** Abscisic acid standardized fig (Ficus carica) extracts ameliorate postprandial glycemic and insulinemic responses in healthy adults. *Nutrients* 11: 1757, 2019. doi:10.3390/nu11081757.

Downloaded from journals.physiology.org/journal/ajpendo (061.197.080.176) on January 24, 2025.

43. **Wan C**, **Yuan T**, **Li L**, **Kandhi V**, **Cech NB**, **Xie M**, **Seeram NP.** Maplexins, new α-glucosidase inhibitors from red maple (Acer rubrum) stems. *Bioorg Med Chem Lett* 22: 597–600, 2012. doi:10.1016/j.bmcl.2011.10.073.
44. **Gai Z**, **Visentin M**, **Gui T**, **Zhao L**, **Thasler WE**, **Häusler S**, **Hartling I**, **Cremonesi A**, **Hiller C**, **Kullak-Ublick GA.** Effects of farnesoid X receptor activation on arachidonic acid metabolism, NF-kB signaling, and hepatic inflammation. *Mol Pharmacol* 94: 802–811, 2018. doi:10.1124/mol.117.111047.
45. **Spector AA.** Arachidonic acid cytochrome P450 epoxygenase pathway. *J Lipid Res* 50, Suppl: S52–S56, 2009. doi:10.1194/jlr.R800038-JLR200.
46. **Spector AA**, **Kim HY.** Cytochrome P450 epoxygenase pathway of polyunsaturated fatty acid metabolism. *Biochim Biophys Acta* 1851: 356–365, 2015. doi:10.1016/j.bbalip.2014.07.020.
47. **Tilg H**, **Adolph TE**, **Dudek M**, **Knolle P.** Non-alcoholic fatty liver disease: the interplay between metabolism, microbes and immunity. *Nat Metab* 3: 1596–1607, 2021. doi:10.1038/s42255-021-00501-9.
48. **Fan Y**, **Pedersen O.** Gut microbiota in human metabolic health and disease. *Nat Rev Microbiol* 19: 55–71, 2021. doi:10.1038/s41579-020-0433-9.
49. **Tripathi A**, **Debelius J**, **Brenner DA**, **Karin M**, **Loomba R**, **Schnabl B**, **Knight R.** The gut-liver axis and the intersection with the microbiome. *Nat Rev Gastroenterol Hepatol* 15: 397–411, 2018 [Erratum in *Nat Rev Gastroenterol Hepatol* 2018]. doi:10.1038/s41575-018-0011-z.
50. **Canfora EE**, **Meex RCR**, **Venema K**, **Blaak EE.** Gut microbial metabolites in obesity, NAFLD and T2DM. *Nat Rev Endocrinol* 15: 261–273, 2019. doi:10.1038/s41574-019-0156-z.
51. **Hiel S**, **Gianfrancesco MA**, **Rodriguez J**, **Portheault D**, **Leyrolle Q**, **Bindels LB**, **Gomes da Silveira Cauduro C**, **Mulders MDGH**, **Zamariola G**, **Azzi AS**, **Kalala G**, **Pachikian BD**, **Amadieu C**, **Neyrinck AM**, **Loumaye A**, **Cani PD**, **Lanthier N**, **Trefois P**, **Klein O**, **Luminet O**, **Bindelle J**, **Paquot N**, **Cnop M**, **Thissen JP**, **Delzenne NM.** Link between gut microbiota and health outcomes in inulin -treated obese patients: lessons from the Food4Gut multicenter randomized placebo-controlled trial. *Clin Nutr* 39: 3618–3628, 2020. doi:10.1016/j.clnu.2020.04.005.
52. **Gibson GR**, **Hutkins R**, **Sanders ME**, **Prescott SL**, **Reimer RA**, **Salminen SJ**, **Scott K**, **Stanton C**, **Swanson KS**, **Cani PD**, **Verbeke K**, **Reid G.** Expert consensus document: The International Scientific Association for Probiotics and Prebiotics (ISAPP) consensus statement on the definition and scope of prebiotics. *Nat Rev Gastroenterol Hepatol* 14: 491–502, 2017. doi:10.1038/nrgastro.2017.75.
53. **Senizza A**, **Rocchetti G**, **Mosele JI**, **Patrone V**, **Callegari ML**, **Morelli L**, **Lucini L.** Lignans and gut microbiota: an interplay revealing potential health implications. *Molecules* 25: 5709, 2020. doi:10.3390/molecules25235709.
54. **Peirotén A**, **Bravo D**, **Landete JM.** Bacterial metabolism as responsible of beneficial effects of phytoestrogens on human health. *Crit Rev Food Sci Nutr* 60: 1922–1937, 2020. doi:10.1080/10408398.2019.1622505.
55. **Gerritsen J**, **Hornung B**, **Renckens B**, **van Hijum SAFT**, **Martins Dos Santos VAP**, **Rijkers GT**, **Schaap PJ**, **de Vos WM**, **Smidt H.** Genomic and functional analysis of Romboutsia ilealis CRIB^T reveals adaptation to the small intestine. *PeerJ* 5: e3698, 2017. doi:10.7717/peerj.3698.
56. **Theilmann MC**, **Goh YJ**, **Nielsen KF**, **Klaenhammer TR**, **Barrangou R**, **Abou Hachem M.** Lactobacillus acidophilus metabolizes dietary plant glucosides and externalizes their bioactive phytochemicals. *mBio* 8: e01421-17, 2017. doi:10.1128/mBio.01421-17.
57. **Lim S**, **Chang DH**, **Ahn S**, **Kim BC.** Whole genome sequencing of "Faecalibaculum rodentium" ALO17, isolated from C57BL/6J laboratory mouse feces. *Gut Pathog* 8: 3, 2016. doi:10.1186/s13099-016-0087-3.
58. **Ke X**, **Walker A**, **Haange SB**, **Lagkouvardos I**, **Liu Y**, **Schmitt-Kopplin P**, **von Bergen M**, **Jehmlich N**, **He X**, **Clavel T**, **Cheung PCK.** Synbiotic-driven improvement of metabolic disturbances is associated with changes in the gut microbiome in diet-induced obese mice. *Mol Metab* 22: 96–109, 2019. doi:10.1016/j.molmet.2019.01.012.
59. **Zhou D**, **Pan Q**, **Xin FZ**, **Zhang RN**, **He CX**, **Chen GY**, **Liu C**, **Chen YW**, **Fan JG.** Sodium butyrate attenuates high-fat diet-induced steatohepatitis in mice by improving gut microbiota and gastrointestinal barrier. *World J Gastroenterol* 23: 60–75, 2017. doi:10.3748/wjg.v23.i1.60.
60. **Bach Knudsen KE**, **Lærke HN**, **Hedemann MS**, **Nielsen TS**, **Ingerslev AK**, **Gundelund Nielsen DS**, **Theil PK**, **Purup S**, **Hald S**, **Schioldan AG**, **Marco ML**, **Gregersen S**, **Hermansen K.** Impact of diet-modulated butyrate production on intestinal barrier function and inflammation. *Nutrients* 10: 1499, 2018. doi:10.3390/nu10101499.
61. **den Besten G**, **Bleeker A**, **Gerding A**, **van Eunen K**, **Havinga R**, **van Dijk TH**, **Oosterveer MH**, **Jonker JW**, **Groen AK**, **Reijngoud DJ**, **Bakker BM.** Short-chain fatty acids protect against high-fat diet-induced obesity via a PPARγ-dependent switch from lipogenesis to fat oxidation. *Diabetes* 64: 2398–2408, 2015. doi:10.2337/db14-1213.

Downloaded from journals.physiology.org/journal/ajpendo (061.197.080.176) on January 24, 2025.